Rev. Roum. Sci. Techn.– Électrotechn. et Énerg.
Vol. **67**, *4*, pp. 371–376, Bucarest, 2022

Électrotechnique et électroénergétique

A NOVEL CONTROL SCHEME IMPLEMENTATION FOR A SELF-EXCITED ASYNCHRONOUS GENERATOR

OUSSAMA ABDESSEMAD[1], AHMED LOKMANE NEMMOUR[1], LAMRI LOUZE[1]

Keywords: Self-excited asynchronous generator; Vector control; Pulse width modulation inverter; Dc-bus voltage regulation; Lead compensator controller design.

This work presents an efficient method for wind power converting applications based on a self-excited asynchronous generator (SEAG). In the adopted study, the machine with the rotor driven by an auxiliary prime mover provides active power to an isolated dc-load via a static converter (SC) associated with a dc bus capacitor through its stator. Thus, for a determined load, the converter's required stator voltages are derived by establishing a specific vector control law relative to a new output control variable introduction. The presented simulation results and their corresponding experimental tests demonstrate that the pretended control strategy ensures perfect output dc-bus voltage tracking performances concerning a simultaneous load drift and the mechanical speed profile.

1. INTRODUCTION

Due to their potential intrinsic advantages, the induction generator IGs constitutes an attractive solution for wind power plants converting applications where the rotor speed is constrained to vary within a specific range [1]. However, these generators must be associated with closed-loop control systems to ensure an output voltage with fixed amplitude and frequency concerning a simultaneous load variation and the mechanical speed profile [2–5].

To satisfy the main core magnetization requirement, the self-excited asynchronous generator (SEAG) configuration requires an external source; this task is conventionally realized by three capacitors connected to stator windings terminals where the voltage build-up process is like paralleled dc generator case.

A single capacitor-static converter (SC) association could also ensure machine magnetization. In this situation, the corresponding magnetization process will have occurred exactly as the conventional use of three-phase capacitors [3–8].

The output voltage terminal regulation task is usually performed by controlling the asynchronous generator's torque and flux quantities separately; several control structures use two paralleled PI control loops, including two cascaded loops; the external loop of the first one is related to the adopted flux regulation and determines the stator current d-axis component set value. Conjointly, the outer loop's task is to ensure the output dc-bus voltage regulation and fixes the stator current q-axis component reference value.

In [3,9–14], various forms of the well-known vector control technique were discussed. A similar solution using the stator flux-oriented control has been proposed in [15]. In [16–19], the proposed solutions that constitute an effective tool for the output dc-bus voltage regulation are based on using stator currents relay controllers. Nevertheless, the rotor flux magnitude is strongly disturbed during transient conditions.

More consistent vector control laws considering the saturation phenomenon are presented in [20,21]; specific dynamical models expressed in magnetizing current components and dynamical inductances are derived. The previous results could be significantly improved, but additional computations inherent to the control structure requirements are needed.

The purpose of this paper is to demonstrate that a reduced version with one control loop of the so-called vector control strategy performed in steady-state conditions using a lead compensator (LC) controller properly tuned can ensure an ideal control performance with an excellent tracking of reference trajectories under simultaneous variations of the dc load and the mechanical speed values.

2. MATHEMATICAL STUDIED SYSTEM MODELING

2.1 MODEL DERIVATION OF INDUCTION GENERATOR

Relative to an orthogonal (d-q) axes rotating with a given velocity ω_s, the induction machine dynamical model is described by the following first-order differential equations with the stator currents and rotor flux components as state variables [22–26]:

$$\begin{cases} V_{sd} = R_s i_{sd} + \dfrac{\mathrm{d}\varphi_{sd}}{\mathrm{d}t} - \omega_s \varphi_{sq} \\ V_{sq} = R_s i_{sq} + \dfrac{\mathrm{d}\varphi_{sq}}{\mathrm{d}t} + \omega_s \varphi_{sd} \\ V_{rd} = R_r i_{rd} + \dfrac{\mathrm{d}\varphi_{rd}}{\mathrm{d}t} - (\omega_s - \omega)\varphi_{rq} \\ V_{rq} = R_r i_{sq} + \dfrac{\mathrm{d}\varphi_{rq}}{\mathrm{d}t} + (\omega_s - \omega)\varphi_{rd} \\ C_{em} = \dfrac{pM}{L_r}\left(i_{sq}\varphi_{rd} - i_{sd}\varphi_{sq}\right) \end{cases} . \quad (1)$$

If the rotor flux vector q-axis component is equal to zero, the above machine model could be explicitly rewritten as [22–26]:

$$V_{sq} = R_s i_{sq} + \sigma L_s \frac{\mathrm{d}i_{sq}}{\mathrm{d}t} + \sigma\omega_s L_s i_{sd} + \omega_s \frac{M}{L_r}\varphi_{rd} . \quad (2)$$

$$\omega_s = \omega + \frac{MR_r}{L_r\varphi_{rd}} i_{sq} = \omega + \frac{M}{T_r\varphi_{rd}} i_{sq} . \quad (3)$$

$$C_{em} = \frac{pM}{L_r} i_{rd}\varphi_{rd} . \quad (4)$$

$$\varphi_{rd} = \frac{M}{1+T_r s} i_{sd} . \quad (5)$$

[1] Laboratoire d'electrotechnique de Constantine (LEC), Université des frères Mentouri, Constantine 1, 25000, Constantine, Algeria, E-mail: oussama.abdessamad@lec-umc.org

Equation (5) shows that the rotor flux d-axis component φ_{rd} follows the stator current d-axis component concerning a first order. In the steady-state conditions, eq. (5) will be reduced to:

$$i_{sd}^{*} = \frac{\varphi_{rd}^{*}}{M}. \quad (6)$$

Now, by replacing eq. (3) and (6) in (2), and by considering φ_{rd} as a constant quantity, the following equation could be obtained:

$$V_{sq} - \varphi_0 \omega = R_{eq} i_{sq} + L_{eq} \frac{\mathrm{d}\, i_{sq}}{\mathrm{d}\, t} = U_{sq}. \quad (7)$$

where $R_{eq} = R_s + L_s/T_r$, $L_{eq} = \sigma L_s$ and $\varphi_0 = L_s \varphi_{rd}^{*} / M$.

One can notice that eq. (7) is analog to a separate dc machine's armature voltage equation.

Equation (7) could be rewritten as:

$$i_{sq}(s) = \frac{1}{R_{eq} + L_{eq} s} U_{sq}(s). \quad (8)$$

Hence, the electromagnetic torque C_{em} formula expressed by eq. (5) could be traduced by:

$$C_{em}(s) = \frac{pM\varphi_{rd}^{*}}{L_r} \frac{1}{R_{eq} + L_{eq} s} U_{sq}(s). \quad (9)$$

Considering that the electromagnetic torque C_{em} has another expression in terms of the stator active power P_s, and the rotor velocity is given by:

$$C_{em} = p \frac{P_s}{\omega}. \quad (10)$$

where p is the pole pair's number.

Consequentially, the stator active power P_s is related to the new voltage quantity U_{sq} as:

$$P_s(s) = \frac{M\varphi_{rd}^{*}}{L_r} \frac{1}{R_{eq} + L_{eq} s} \omega(s) U_{sq}(s). \quad (11)$$

Equation (11) shows that for a given rotor speed, it is possible to govern the stator active power P_s by acting on the voltage quantity U_{sq} via an appropriate design of a lead compensator controller.

2.2 SEAG-SC-DC BUS SYSTEM MATHEMATICAL MODELING

The studied wind-power conversion structure is based on a self-excited asynchronous generator (SEAG) entrained by a wind turbine and supplying an isolated dc load via a three-phase static converter with an output capacitor. Figure 1 gives the corresponding per-phase association scheme.

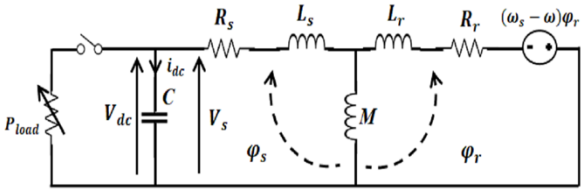

Fig. 1 – The per-phase SEAG-SC association.

The active power P_{load} absorbed by the load is related to the machine stator powers P_s and the dc-bus power P_{dc} [9, 12] by:

$$P_{dc} = P_s - P_{load}. \quad (12)$$

The power P_{dc} could be also expressed in terms of the current traversing the capacitor and the voltage across this later by:

$$P_{dc} = V_{dc} i_{dc} = V_{dc} C \dot{V}_{dc}, \quad (13)$$

where C denotes the capacitor value.

The Laplace form corresponding to eq. (13) is:

$$P_{dc}(s) = V_{dc} i_{dc} = C s V_{dc}^2(s). \quad (14)$$

This yields to:

$$C s V_{dc}^2(s) = P_s(s) - P_{load}(s). \quad (15)$$

One can conclude from eq. (15) that the dc-bus voltage square value V_{dc}^2 is completely governed by the stator active power P_s against the load power P_{load} variations that act as a disturbance. The combination of eq. (11) and (15) under the assumption $P_{load} = 0$ give:

$$Cs \frac{V_{dc}^2(s)}{\omega(s)} = \frac{M\varphi_{rd}^{*}}{L_r} \frac{1}{R_{eq} + L_{eq} s} U_{sq}(s). \quad (16)$$

By adopting the quotient $Y(s) = V_{dc}^2(s) / \omega(s)$ as a new output variable, eq. (16) becomes:

$$Y(s) = \frac{K}{s(R_{eq} + L_{eq} s)} U_{sq}(s). \quad (17)$$

with: $K = M\varphi_{rd}^{*} / CL_r$.

3. THE OUTPUT DC-BUS VOLTAGE REGULATION STRATEGY

3.1 THE DC-BUS VOLTAGE CONTROLLER DESIGN

Equation (17) shows that the new variable adopted $Y(s)$ which contains the output dc-bus voltage V_{dc} is effectively controlled by the U_{sq} voltage defined by eq. (7) according to the closed-loop control of Fig. 2.

The suggested control method aims to realize an output dc-bus voltage under an electrical variable rotor speed via the control of the new variable defined by:

$$Y(s) = \frac{V_{dc}^2(s)}{\omega(s)} \quad (18)$$

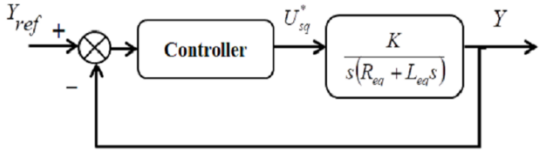

Fig. 2 – The new variable Y closed-loop control.

For this purpose, a typical design of a lead compensator (LC) where the dominant pole characterizing the closed-loop transfer function is placed $s = (-1 + j\sqrt{3}) / T_{eq}$ will be conducted. Under these considerations, the total of the phase contributions of the open-loop transfer function poles (at $s = 0$ and $s = -R_{eq} / L_{eq} = -1/T_{eq}$) according to Fig. 3 (a) is given by:

$$-120° - 90° = -210°.$$

For this closed-loop transfer function poles configuration relative to the above choice, an angle value 30° must be

added to the open-loop transfer function's poles location.

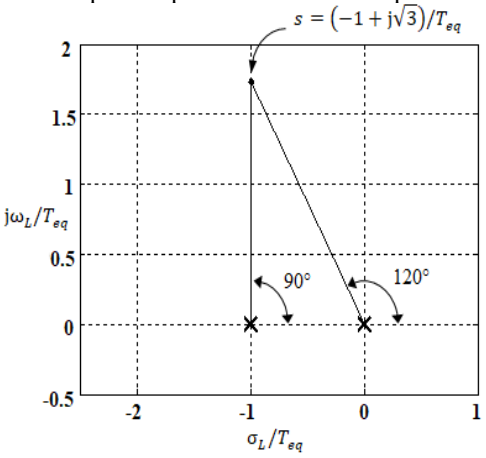

Open-loop poles and the closed-loop transfer functions desired poles.

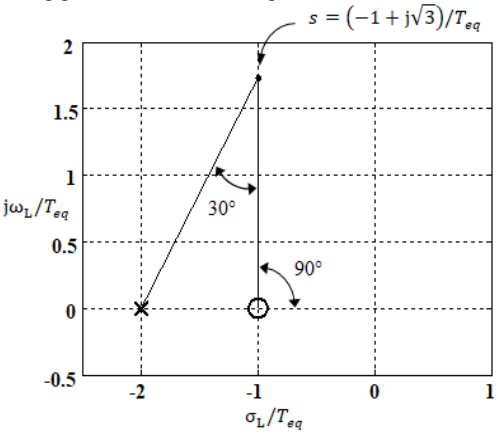

Compensator phase design for a 30° contribution lead angle.

Fig. 3 – The adopted output Y closed-loop control.

Consequently, the total angle insufficiency of the given open-loop transfer function concerning the desired closed-loop pole $s=\left(-1+j\sqrt{3}\right)/T_{eq}$ is evaluated as [27]:

$$180°-120°-90°=-30°. \tag{20}$$

In this case, the control procedure relative to the compensator design must provide 30° which corresponds to a lead compensator (LC) class.

The corresponding standard form of this controller is:

$$G_c(s)=g\frac{s+a}{s+b}. \tag{21}$$

If the zero of the lead compensator choice is made for $s=-1/T_{eq}$, the corresponding pole of the compensator will be situated $s=-2/T_{eq}$ to have a resulting phase lead angle of 30° (Fig. 3). In this case, eq. (21) becomes:

$$G_c(s)=g\frac{s+1/T_{eq}}{s+2/T_{eq}}. \tag{22}$$

The constant g is determined from the steady-state conditions verifying:

$$\left|g\frac{s+1/T_{eq}}{s+2/T_{eq}}\frac{K}{s\left(R_{eq}+L_{eq}s\right)}\right|_{s=\left(-1+\sqrt{3}\right)/T_{eq}}=1. \tag{23}$$

Under these conditions, the resultant open-loop transfer function $G_{comp}(s)$ of the compensated system is given by:

$$G_{comp}(s)=G_c(s)\frac{K/L_{eq}}{s\left(s+1/T_{eq}\right)}=\frac{gK/L_{eq}}{s\left(s+2/T_{eq}\right)}. \tag{24}$$

For the considered machine data shown in Table 1, the corresponding equivalent time constant is $T_{eq}=0.0036$ s.

In this case, the controller's transfer function is:

$$G_c(s)=7.94\frac{s+263.16}{s+526.32}. \tag{25}$$

By referring to Fig. 4 (a), the closed-loop transfer function of the initial system with unity feedback relative to the considered machine data is:

$$\left.\frac{Y(s)}{Y_{ref}(s)}\right|_{\substack{original\\system}}=\frac{1758.9}{s^2+262.6s+1758.9}. \tag{26}$$

The compensated system's closed-loop transfer function is:

$$\left.\frac{Y(s)}{Y_{ref}(s)}\right|_{\substack{compensed\\system}}=\frac{13948.08}{s^2+526.32s+13948.08}. \tag{27}$$

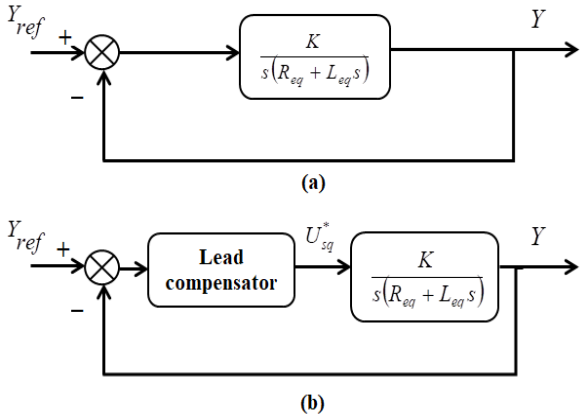

Fig. 4 – The adopted setting output Y by considering a unity feedback system.

The step response of the initial and compensated system's behaviors is shown in Fig. 5.

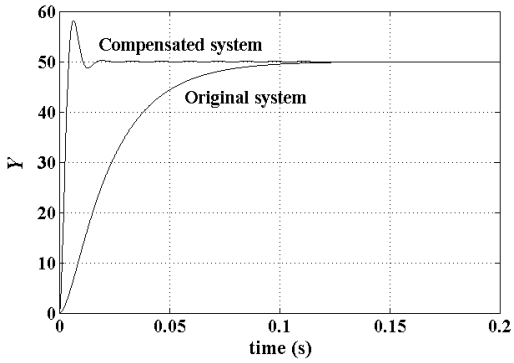

Fig. 5 – The Y step response with the used LC controller.

3.2 THE STATOR VOLTAGE Q-AXIS COMPUTATION

The stator voltage q-axis component V^*_{sq} is obtained from the new variable Y controller output U^*_{sq} as:

$$V_{sq}^{*}(k)=U_{sq}^{*}(k)+\frac{L_S}{M}\varphi_{rd}^{*}\omega(k). \quad (28)$$

Considering that the SEAG is operating in steady-state conditions of the vector control strategy, the stator pulsation quantities ω_s^* and the voltage d-axis component V_{sd}^* are respectively given by:

$$\omega_s^{*}(k)=\omega(k)+\frac{M}{T_S\varphi_{rd}^{*}}\hat{i}_{sq}(k). \quad (29)$$

$$V_{sd}^{*}(k)=\frac{R_S}{M}\varphi_{rd}^{*}-L_{eq}\omega_s(k)\hat{i}_{sq}(k). \quad (30)$$

4. SIMULATION VERSUS PRACTICAL TESTS RESULTS

The detailed control strategy concerning the self-excited asynchronous generator (SEAG) is initially tested by performing software simulation software of a 1.5 kW, 380 V, and 50 Hz wound rotor asynchronous machine (Table 1). The output dc-bus voltage regulation has been realized through the proposed quantity Y control with the LC controller design by considering a variable Y_{ref} profile set value and dc load.

Table 1

Parameters values of the used IG

Parameter description	Value
Rated power	1.5 kW
Rated voltage	380 V
Rated frequency	50 Hz
Pole-pairs number	2
Stator resistance	4.700 Ω
Stator inductance	0.395 H
Rotor resistance	0.500 Ω
Rotor inductance	0.023 H
Mutual inductance	0.089 H

The proposed control scheme and the corresponding experimental setup test bench are presented in Fig. 6 and 7, respectively. An experiment test bench with a Dspace-DS1104 control board has been implemented to validate the proposed regulation concept. The asynchronous generator stator windings terminals are coupled to the output dc bus via a three-phase voltage source IGBT inverter. An LV 100–500 voltage sensor with a 1024 pulses incremental encoder is used for the dc-bus voltage and the rotor velocity acquisitions performed at each 0.1 ms sampling time.

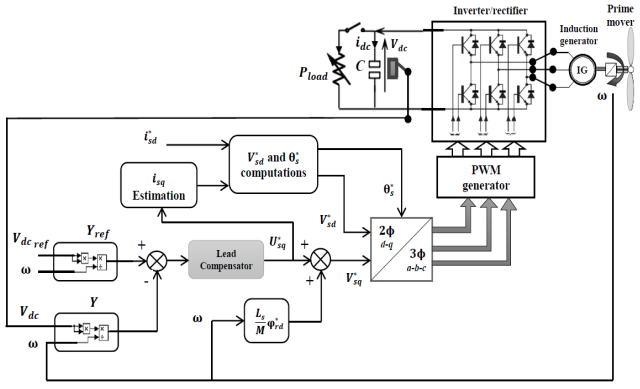

Fig. 6 – The suggested dc-bus voltage regulation layout.

Simulation and experimental tests of the proposed control strategy were carried out in identical conditions. The time response of a step-changing dc-bus voltage from 250 V to 300 V introduced at t = 9.5 s after the load introduction P_{load} = 800 W at t = 2.4 s is presented in Fig. 8. The proposed regulation procedure relative to the lead compensator controller designing procedure ensures a perfect rejection of the imposed load-power with an excellent output dc-bus voltage tracking performance.

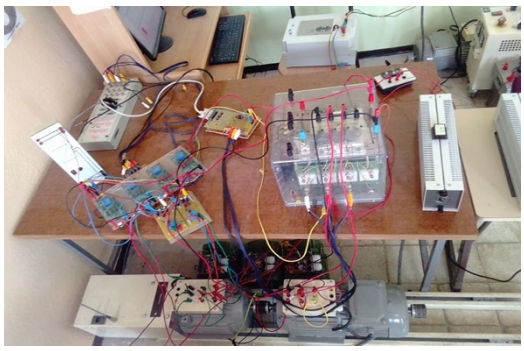

Fig. 7 – The complete test bench implementation.

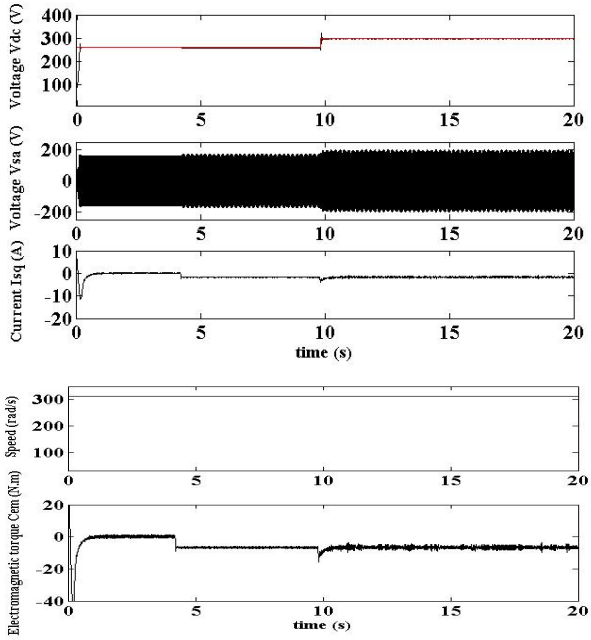

(a) Simulation results

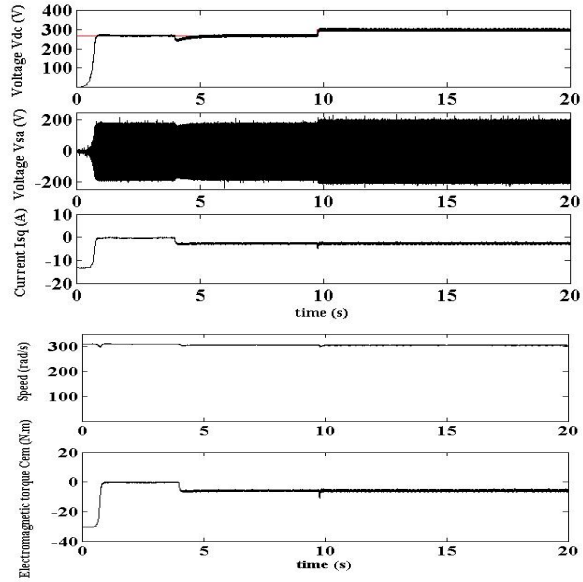

b) Practical results

Fig. 8 – The proposed SEAG control performances.

To emulate the practical situation where the SEAG rotor is coupled to a wind turbine, a variable speed profile of the dc motor is adopted. Figure 9 shows that the tracking performances of the proposed power conversion system control are not influenced by the rotor speed fluctuations.

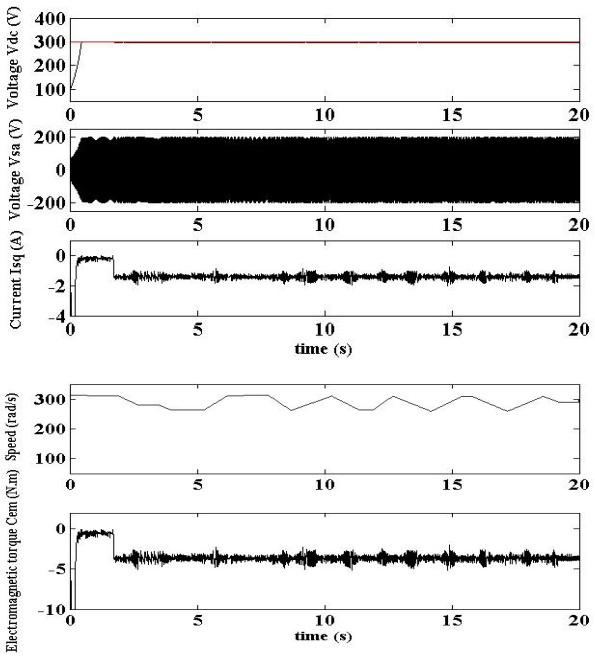

(a) Simulation results

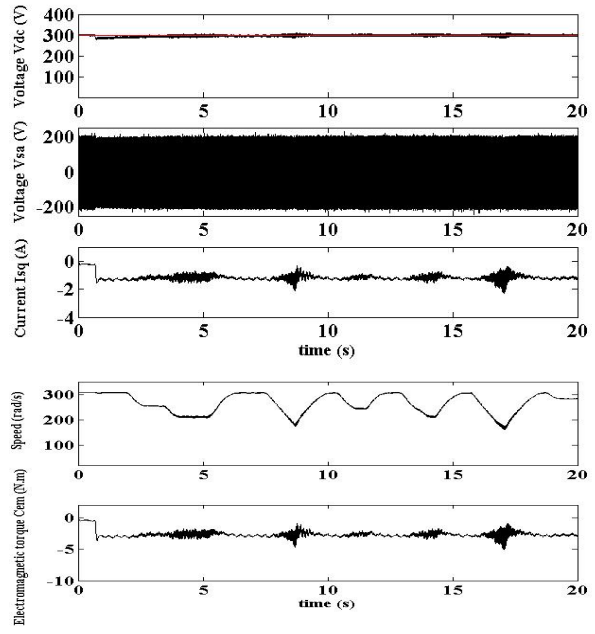

(b) Practical results

Fig. 9 – Responses of IG control under the variation of rotor speed.

5. CONCLUSIONS

This article presents a detailed control strategy for an isolated induction generator based on a reduced rotor field orientation technique. By referring to the new output control quantity adopted, the resulting control scheme gives the required control quantities analogously to the separated dc machine case. Experiment results approve the effectiveness of the proposed solution with perfect tracking performances of the dc-bus voltage value by using a lead compensator with a typical parameter sizing method. The global control behavior is checked by considering principal external disturbances such as the load-power demand and the rotor speed variations. Wind power conversion plants could easily exploit the studied control system conversion.

Received on 21 December 2021

REFERENCES

1. G.K. Singh, *Self-excited induction generator for renewable applications*, Encyclopedia of Sustainable Technologies, Elsevier, 2017, pp. 239–256 (2017).
2. K. Charafeddine, K. Sangov, S. Tsyruk, *Automatic voltage regulation and stability analysis of three-phase self-excited induction generator for wind energy*, IEEE 2nd Int. Conf. on the Applications of Information Technology in Developing Renewable Energy Processes & Systems, Amman, Jordan, Dec. 6-8, 2017.
3. J. Mishra, M. Pattnaik, S. Samanta, *Performance evaluation of a self-excited induction generator for stand-alone wind energy conversion system*, IEEE Power, Communication and Information Technology Conf., Bhubaneswar, India, Oct. 15-17, 2015.
4. A. Aberbour, K. Idjdarene, A. Tounzi, *Sliding mode direct torque and rotor flux control of an isolated induction generator including magnetic saturation*, Rev. Roum. Sci. Techn. – Électrotechn. Et Énerg., **61**, 2, pp. 142–146 (2016).
5. R. Mishra, T.K. Saha, *Development of a standalone VSCF generation scheme through three stage control of SCIG*, IEEE Region 10 Conference (TENCON), 22-25 Nov. 2016.
6. L.A. Lopes, R.G. Almeida, *Wind-driven self-excited induction generator with voltage and frequency regulated by a reduced-rating voltage source inverter*, IEEE Trans. on Ener. Conver., **21**, *2*, pp. 297–304 (2006).
7. J.K. Chatterjee, B.V. Perumal, N.R.Gopu, *Analysis of operation of a self-excited induction generator with generalized impedance controller*, IEEE Transactions on Energy Conversion, **22**, *2*, pp. 307–315 (2007).
8. Z. Boudries, A. Aberbour, K. Idjdarene, *Study on sliding mode virtual flux-oriented control for three-phase PWM rectifiers*, Rev. Roum. Sci. Techn. – Électrotechn. Et Énerg., **61**, *2*, pp. 153–158 (2016).
9. O. Abdessemad, A.L. Nemmour, L. Louze, A. Khezzar, *An experiment validation of an efficient vector control strategy for an isolated induction generator as wind power conversion*, IEEE International Conference on Advanced Electrical Engineering, (ICAEE), Algiers, Algeria, Nov. 19-21, 2019.
10. S.M. Mahato, S.P. Singh, M.P. Sharma, *Direct vector control of stand-alone self-excited induction generator*, Joint International Conference on Power Electronics, Drives and Energy Systems & 2010 Power India, New Delhi, India, Dec. 20-23, 2010.
11. S. Hazra, P. Sensarma, *Vector approach for self-excitation and control of induction machine in stand-alone wind power generation*, IET renewable power generation, **5**, *5*, pp. 397–405 (2011).
12. O. Abdessemad, A.L. Nemmour, L. Louze, A. Khezzar, *Real-Time Implementation of a Novel Vector Control Strategy for a Self-Excited Asynchronous Generator Driven by a Wind Turbine*, Journal Européen des Sys. Automatisés, **54**, *2*, pp. 235–241 (2021).
13. T. Ahmed, K. Nishida, M. Nakaoka, *Advanced voltage control of induction generator using rotor field-oriented control*, Fortieth IAS Annual Meeting. Conference Record of the 2005 Industry Applications Conference, Hong Kong, China, Oct. 2-6, 2005.
14. N.P. Quang, J.A. Dittrich, *Vector Control of Three-Phase AC Machines: System Development in the Practice.* Berlin, Heidelberg: Springer (2008).
15. D. Seyoum, M.F. Rahman, C. Grantham, *Terminal voltage control of a wind turbine driven isolated induction generator using stator-oriented field control*, Eighteenth Annual IEEE Applied Power Electronics Conf. and Exposition, FL, USA, Feb. 9-13 2003.
16. A.L. Nemmour, L. Louze, A. Khezzar, M. Boucherma, *Terminal Voltage Control of Variable Speed Induction Generator Driven by a Wind Turbine Supplying a DC Load*, International Aegean Conference on Electrical Machines and Power Electronics, Bodrum, Turkey, Sept. 10-12, 2007.
17. S.S. Kumar, N. Kumaresan, M. Subbiah, M. Rageeru, *Modelling, analysis and control of stand-alone self-excited induction generator-pulse width modulation rectifier systems feeding constant DC voltage applications*, IET Generation, Transmission

& Distribution, **8**, *6*, pp. 1140–1155 (2014).
18. S.A. Deraz, F.A. Kader, *A new control strategy for a stand-alone self-excited induction generator driven by a variable speed wind turbine*, Renewable Energy, **51**, pp. 263–273 (2013).
19. L. Louze, O. Abdessemad, A.L. Nemmour, A. Khezzar, *An effective control of an isolated induction generator supplying DC load for wind power converting applications*, Electrical Engineering and Electromechanics, **3**, pp. 65–69 (2020).
20. S. Meddouri, K. Idjdarene, L. Ferrarini, *Control of autonomous saturated induction generator associated to a flywheel energy storage system*, Rev. Roum. Sci. Techn. – Électrotechn. Et Énerg., **61**, *4*, pp. 372–377 (2016).
21. E. Margato, J. Faria, M.J. Resende, J. Palma, *A new control strategy with saturation effect compensation for an autonomous induction generator driven by wide speed range turbines*, Energy Conversion and Management, **52**, *5*, pp. 2142–2152 (2011).
22. F. Amrane *et al.*, *Design and implementation of high performance field oriented control for grid-connected doubly fed induction generator via hysteresis rotor current controller*, Rev. Roum. Sci. Techn. – Électrotechn. Et Énerg., **61**, *4*, pp. 319–324 (2016).
23. O. Bachir, A.F. Zoubir, *Comparative analysis of robust controller based on classical proportional-integral controller approach for power control of wind energy system*, Rev. Roum. Sci. Techn. – Électrotechn. Et Énerg., **63**, *2*, pp. 210–216 (2018).
24. W. Leonard *Control of Electrical Drives*, New York: Springer. 1985.
25. P. Vas *Vector Control of AC Machines*. Oxford, U.K.: Oxford University Press, 1990.
26. A. Kerboua, M. Abid, *Hybrid fuzzy sliding mode control of a doubly-fed induction generator in wind turbines*, Rev. Roum. Sci. Techn. – Électrotechn. Et Énerg., **57**, *4*, pp. 412–421 (2012).
27. R.V. Dukkipati, *Analysis and Design of Control Systems Using MATLAB*, Connecticut, USA: New Age International, 2006.